ESTIMATE OF DISCHARGE RATES IN NANEDI VALLIS, MARS. H. Gregoire-Mazzocco[1], N. Mangold[1], F. Costard[1], V. Ansan[1], P. Masson[1], G. Neukum[1] and the HRSC Team, [1]*IDES, Bât. 509, Université Paris XI, 91405 Orsay cedex*, [2]*Institut für Geologische Wissenschaften, Freie Universität Berlin, Germany*, *(contact: gmh7@geol.u-psud.fr).*

Introduction. Previous studies have shown signs of a sustained fluvial activity in the Xanthe Terra region on Mars, it is cut by several valley systems which formation processes still remain controversial regarding the relative roles of groundwater sapping and surface runoff. We focus our study on the 800-km long Nanedi Vallis. Its highly sinuous shape and the presence of a small channel on the valley floor strongly indicates an origin by slow erosion of running water, and the lack of tributaries suggests that the river that cut the valley was mainly fed by groundwater [**1**]. Using the High Resolution Stereo Camera (HRSC) data we perform a morphometric analysis of the valley. The results are used in two different approaches to estimate the discharge rates . The purpose of this study is to find out wether or not the overall shape of the valley can be explained by the characteristics of the interior channel observed and thus if it is the result of continual fluid flow.

Data and Methods. Although interior channel in a portion of Nanedi Vallis has already been identified in a MOC image [**2**], data commonly used to study the entire valley (MOLA, Viking) do not offer a high enough spatial resolution to determine precisely the morphometric properties of such large feature. The HRSC images cover areas as large as $\sim 3 \times 10^5 km^2$ with a spatial resolution of typically $12-20m/pixel$ [**3**]. It also provides Digital Terrain Models (DTM) derived from the stereo images. HRSC acquired three adjacent images strips (Mars Express orbits 894, 905 and 927) that offer a total coverage of Nanedi Vallis at a resolution of $\sim 13 - 23m/pixel$ (Fig. 1). We would like to insist on the difference between the entire canyon which, in this study, will also be referred to as the valley and the interior channels.

After the extraction of the the valley from HRSC image 0905, its centerline was computed to characterize the geometry using a theoretical framework used in the analysis of meandering rivers [**4**]. A meander is defined as a portion of the valley containing three consecutive inflection points. For each meander we define the intrinsic wavelength, L_s, computed along the the centerline, the cartesian wavelength, L, defined by the distance between the initial and the terminal points of the meander. The degree of meandering is measured by the dimensional parameter "sinuosity," defined as $\sigma = L_s/L$. All together 66 individual meanders were identified. Distributions of sinuosity and meander wavelengths were calculated for the entire length of the valley (Fig. 2). We selected two sites, with different characteristics, where the interior channel was observable. Site 1 (312^o.3E, 7^o.6) is located in the last portion of Nanedi Vallis where the two branches meet and we can observe that the valley gets narrower and less sinuous. On the other hand, Site 2 (311^o.8E, 5^o.2), is located in the right branch, the most sinuous portion of Nanedi vallis (Fig. 1).

Although there is usually no obvious link between the sinuosity of a valley and of its interior channel, we observed that, in the 2 sites described, inner channels follow the same path as the whole valley, thus have same wavelength and sinuosity. Based on this observation, we calculated discharge rates at both sites using 2 approaches in order to look for consistency between the overall morphology of the canyon and the characteristics of interior channels.

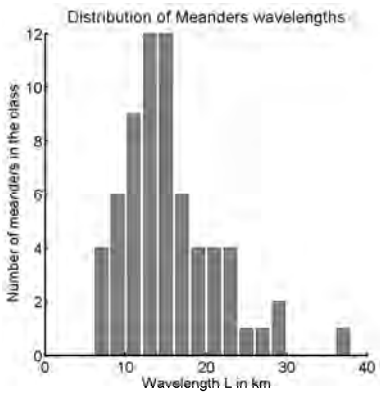

Figure 2: The distribution of meanders wavelengths indicates a dominant wavelength for Nanedi Vallis $Ldom \sim 14km$.

The first method (Method 1) we used is an empirical relationship that links meander wavelength to the bankfull discharge: $L = k\sqrt{Q}$, where k is typically 54.3 on Earth [**5**], and should be rescaled to $kg^{-1/4}$, g being the relative gravity (0.38), to take into account Martian Gravity.

To estimate the bankfull discharge from the characteristics of the interior channels we used a modified Manning equation that takes into account the effects of gravity (Method 2):

$$Q = HWV = H^{5/3}S^{1/2}g^{1/2}Wn^{-1}$$

where H is the mean flow depth, W is the channel width, V is the mean velocity, S is slope, g is again the relative gravity, and n is the Manning roughness coefficient [**6, 7**].

Results. For the 66 meanders the range of L is $6.45 \times 10^3 - 3.75 \times 10^4$ m, the range of L_s is $1.15 \times 10^4 - 4.55 \times 10^4$ m. The range of σ is 1.12 to 2.70, with $\langle\sigma\rangle = 1.41$ and $\langle(\sigma - \langle\sigma\rangle)^2\rangle^{1/2} = 0.11$. In Fig. 2 the distribution of L shows that the dominant wavelength is $Ldom \sim 14km$. We used this value in method 1 to estimate an average value of bankfull discharge for the entire Valley, we obtained $Q \sim 4.1 \times 10^4 m^3 s^{-1}$.

We estimated the various parameters needed for both methods at each test site. Inner channel 1 is part of a meander that has a sinuosity $\sigma_1 = 1.17$ and a wavelength $L_1 = 22690m$. Its width was measured from HRSC image 0905 : $W_1 = 336m$. Assuming a typically observed width to depth ratio $\beta = 10$ we estimated $H \sim 33m$. The average slope was obtained from MOLA, we found $S = 0.002$. Inner channel 2

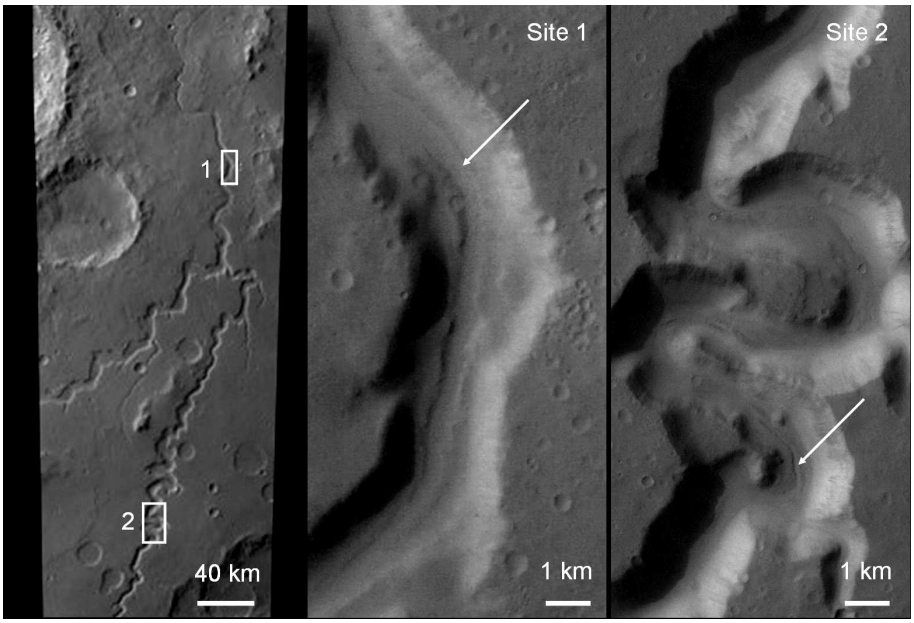

Figure 1: A portion of the HRSC image from orbit h0905 showing Nanedi Vallis. The center of the image is at $\sim 311^o$8E, 7^o2. The areas in the white frames are shown at HRSC resolution ($\sim 15m/pixel$) on the right images. It shows Site 1 and Site 2 where the arrows point to the interior channels observable at the bottom of the valley.

is characterized by $\sigma_1 = 2.64$, $L_2 = 6475m$, $W_2 = 175m$, $H \sim 17m$ and $S = 0.001$. Table 1 shows the value of bankfull discharge at each test site, for the 2 methods described previously.

Location	Site 1	Site 2
Discharge from Method 1	$Q_1 = 10.7 \times 10^4$	$Q_2 = 8.8 \times 10^3$
Discharge from Method 2	$Q_{1man} = 9.6 \times 10^4$	$Q_{2man} = 11.9 \times 10^3$

Table 1: Estimate of bankfull discharges obtained using 2 different methods at Sites 1 and 2, results are expressed in m^3s^{-1}.

Discussion. We find that there is a good agreement between the two methods used to estimate bankfull dicharges: $Q_1 = 10.7 \times 10^4 m^3 s^{-1}$ and $Q_{1man} = 9.6 \times 10^4 m^3 s^{-1}$ at Site 1, $Q_2 = 8.8 \times 10^3 m^3 s^{-1}$ and $Q_{2man} = 11.9 \times 10^3 m^3 s^{-1}$ at Site 2. This indicates that the interior channel observed in Nanedi Vallis might have been carved by flows of characteristics similar to the original channel that formed the canyon.

The values obtained at site 1 are in the range of the bankfull discharges observed for the Lena river in Russia ($\sim 7.4 \times 10^4 m^3 s^{-1}$) and the Amazon in Brazil ($\sim 21.2 \times 10^4 m^3 s^{-1}$). They are a factor $\sim 2-6$ smaller than discharges estimated in interior channels in Lybia Montes, where Jaumann et al. found $Q_{bf} \sim 22 - 68 \times 10^4 m^3 s^{-1}$ [**7**]. Such differences can be explained by the topography: the average slope in Lybia Montes is $S = 0.01$, whereas at site 1 we estimated $S = 0.002$. Site 2 yields values in the range of terrestrial rivers like the Nile ($Q_{bf} \sim 9.8 \times 10^3 m^3 s^{-1}$) or the Niger ($Q_{bf} \sim 12 \times 10^3 m^3 s^{-1}$).

We observe a significant difference in the sinuosity, and consequently in the discharges estimated, between the two test sites. Although further analysis will be needed to conclude definitely, it is possible to argue that there are mainly two reason for this difference: first, the average slope in Site 1 is twice as the slope in Site 2, second, Site 1 is located after the junction of the two branches of Nanedi vallis, explaining the gain of discharge and the diminution of sinuosity.

Ongoing investigations focus on linking those results with a more precise topographic analysis in order to assess the duration of fluvial activity responsible for the formation of Nanedi Vallis.

References. **(1)**. Malin, M.C. and Carr, M.H. (1999), *Nature, 397*, 588-591.**(2)**. Malin, M.C., and Edgett, K.S. (1998) *Lunar and Planetary Science XXXI*, # 1189. **(3)**. Neukum et al.(2004), *J. Fluid Mech., 162*, 139-156. **(4)**. Marani, M. et al. (2002), *Water Resour. Res. 38*, 1225. **(5)**. Mount, J. (1995), *California Rivers and Streams*, Univ. of Cal. press. **(6)**. Irwin III, R.P. et al. (2005) *Geology, 33(6)*, 489-492. **(7)**. Jaumann R. et al (2005), *GRL, 32*, L16203.